Image flickering-free polymer stabilized fringe field switching liquid crystal display

YINGFEI JIANG,[1] GUANGKUI QIN,[2] XIAOGUANG XU,[2] LI ZHOU,[2] SEUNGHEE LEE,[3] AND DENG-KE YANG[1,*]

[1]*Chemical Physics Interdisciplinary Program, Liquid Crystal Institute, Kent State University, Kent, Ohio 44242, USA*
[2]*BOE Technology Group Co., No. 9 Dize RD, BDA, Beijing 100171, China*
[3]*Department of Polymer Nano-Science and Technology, Chonbuk National University, Jeonju, Jeonbuk 561-756, South Korea*
*dyang@kent.edu

Abstract: Liquid crystal displays are the leading technology for flat panel displays. Their energy efficiency is low, however, due to the light absorption caused by polarizers and color filters and power consumption by driving circuitries. In displaying static images, their energy efficiency can be improved if a low driving frequency is used. As the driving frequency is decreased, the transmittance of the displays may change with time, a phenomenon known as image flickering. In this research we demonstrated that polymer stabilization can significantly reduce the flickering in fringe field switching (FFS) liquid crystal display. Under the polymer stabilization, the driving voltage remains low and the response time becomes shorter. Through simulation study, we find that the polymer stabilization smooths the spatial variation of the liquid crystal orientation in the display, and thus reduce the flexoelectric effect which is responsible for image flickering. The polymer stabilization can be implemented in the current main stream manufacturing to produce displays that can show static images under low power consumption.

1. Introduction

Liquid crystal displays (LCDs) are the leading technology for flat panel displays and are widely used in many applications from small-size devices, such as smartphones, to large-screen devices such as TVs [1–3]. The most common display modes are twist nematic (TN) [4], vertical alignment (VA) [5–7], in-plane-switch (IPS) [8–11], fringe field switch (FFS) and ADvanced Super Dimension Switch (ADS) [12,13]. Their energy efficiency is, however, low due to light absorption caused by polarizers and color filters and power consumption by the driving circuitry. LCDs are addressed frame by frame. The voltage applied changes polarity from one frame to the next frame in order to avoid liquid crystal degradation caused by electrochemical reactions under DC voltage in prolonged time. The time interval of a frame is the frame time. The inversion of the frame time is the driving frequency. The power consumption of the driving circuitry is proportional to the driving frequency. One way to improve the energy efficiency is to use low driving frequency. In many applications, such as Ebook and electronic sign board, the displayed images are changed slowly or static, and thus low driving frequencies can be used to save energy. As the driving frequency is decreased, however the transmittance of the display (and thus the brightness of the image) may change with time, a phenomenon known as image flickering [14–23]. There are two factors responsible for the flickering. One of the factors is the low resistivity of the LC material, which makes the voltage across the LC decrease during each frame. The other factor is the flexoelectric effect of the LC [3,24–32], whose aligning effect on the LC is sensitive to the polarity of the applied voltage. When the polarity of the applied voltage is changed from one frame to the next frame, the orientation of the LC changes, which results in a change of the

transmittance of the display, even though the amplitudes of the voltage in the two frames are the same.

There have been many efforts to reduce the flickering. For example, Kim et al. doped bent-core materials into nematic LC hosts to reduce the flexoelectric coefficient [19]. Oh et al. applied a bipolar voltage, instead of a unipolar voltage, to reduce the flexoelectric effect [20]. They also suggested to use electrode spacing to control the flickering [21]. In this paper we report a different approach where polymer stabilization is used to reduce the flickering caused by the flexoelectric effect. A small amount of polymer network is dispersed in the LC, which smooths the LC director configuration under externally applied electric fields. It significantly reduces the flexoelectric effect.

2. Experiment and results

The liquid crystal display mode under study is the fringe field switch (FFS) mode which has a superior performance and is widely used for TVs and smartphones such as Apple Iphones. The structure of the FFS mode is schematically shown in Fig. 1. The rubbing direction of the alignment layer makes the angle of 11° with respect to the pixel stripe electrode. The electrode width and gap are 3 μm and 5 μm, respectively, and the cell thickness is 4.5 μm.

In the voltage-off state, the LC is uniformly aligned parallel to the alignment layer rubbing direction which is parallel to the transmission axis of the bottom polarizer as shown in Fig. 1(a). When the incident light propagates through the LC layer, its polarization remains unchanged; it is then absorbed by the top polarizer whose transmission axis is orthogonal to that of the bottom polarizer. In the voltage-on state, the LC molecule is reoriented by the electric field as shown in Fig. 1(b). When the incident light propagates through the LC layer, its polarization changes; and then passes the top polarizer.

Polymer stabilization has been used to stabilize LC states and improve the performance of liquid crystal devices [34–38]. In this method a small amount of mesogenic monomer is mixed with the LC. The mixture is filled into the LC cell and then photo-polymerized. The cell is irradiated by UV light to photo-polymerize the monomer. When the monomer is polymerized, it forms an anisotropic polymer network which mimics the structure of the LC state. The polymer network has a strong aligning effect on the LC.
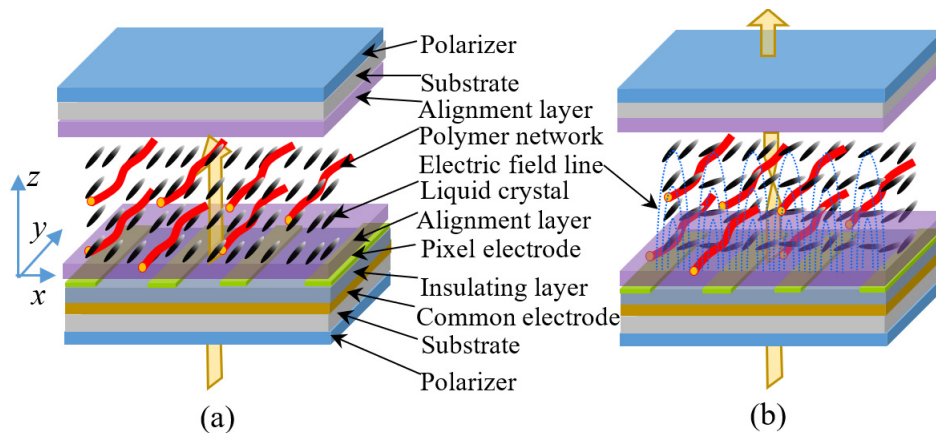

Fig. 1. Schematic diagram of FFS mode, (a) Voltage-off state, (b) Voltage-on state

In our experiment, the LC host is MAT-11575 ($\Delta\varepsilon = 5.5$, $\Delta n = 0.1157$, Merck). This material has a very high resistivity, thus the ionic effect is negligible. The monomer is a bifunctional mesogenic RM257 (Merck). The photo-initiator is Irgacure 651(Ciba), whose concentration is about 5% of the monomer. The mixture is filled into the FFS cell under capillary action in the isotropic phase at an elevated temperature. The transmittance of the cells is defined as the ratio between the intensity of light passing the cells and the intensity of

light passing two polarizers with parallel transmission axes. Then the cell is irradiated under UV light (produced by a high pressure Mercury lamp) with the intensity of 6 mW/cm^2 for 30 m at room temperature and without applied voltage to polymerize the monomer. After polymerization, the formed polymer network is parallel to the alignment layer rubbing direction as shown in Fig. 1 and tends to keep the LC in this direction. The electro-optical properties of the cell under the influence of the polymer network are measured. In the measurement of the electro-optical response of the cells, a He-Ne green laser with wavelength of 543 nm is used.

In order to study the effect of the polymer network, we prepare four mixtures with the monomer concentrations of 0%, 1%, 2% and 3%, respectively. The mixtures are filled into four FFS cells. The transmittance-voltage curves of the cells before the polymerization are shown in Fig. 2(a). The frequency of the applied voltage is 1 kHz under which the flickering is very small. The monomer has little effect on the electro-optical properties. The transmittance-voltage curves of the cells are almost identical, independent of the monomer concentration. The maximum transmittance T_{max} of 42% is obtained at 7 V. We choose the voltage 2.6 V, at which the transmittance is 20% of the maximum transmittance T_{max} to study the flickering. When a square wave voltage with the amplitude of 2.6 V and the frequency of 5 Hz is applied to the cells, their transmittance-time curves are measured. The results are shown in Fig. 2(b). The flickering is large that the transmittance varies considerably with time. The transmittance is sensitive to the polarity of the applied voltage. The transmittance is high when the polarity of
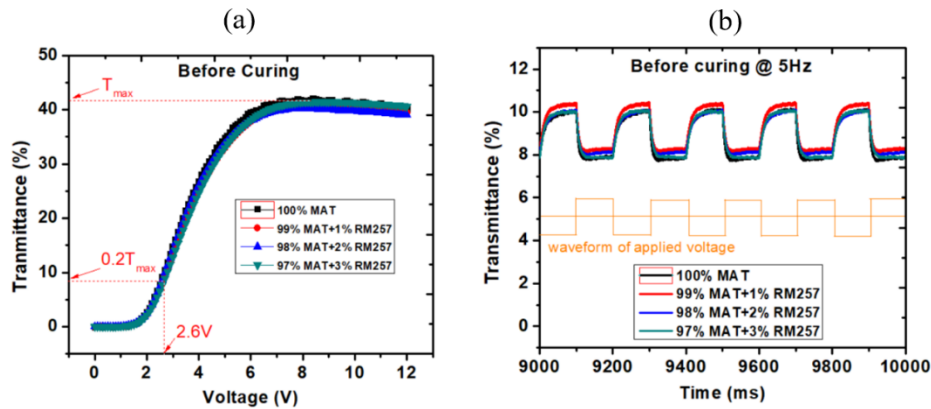

Fig. 2. Electro-optical properties before polymerization of the FFS cells with various polymer concentrations. (a) Transmittance-voltage curves, (b) Transmittance-time curves.

the applied voltage is negative. In order to quantitatively discuss the flickering, we use the flickering value which is defined by

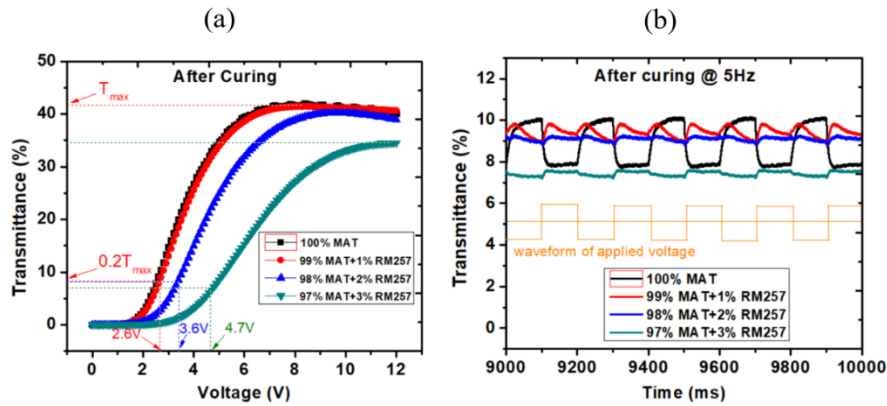$$F = \frac{(T_h - T_l)}{[(T_h + T_l)/2]},\qquad(1)$$

Fig. 3. Electro-optical properties after polymerization of the FFS cells with various polymer concentrations. (a) Transmittance-voltage curves, (b) Transmittance-time.

where T_h and T_l are the highest and lowest transmittance, respectively, under the applied voltage wave. When the applied voltage is + 2.6 V, the highest transmittance is $T_h = 10.1\%$. When the applied voltage is −2.6 V, the highest transmittance is $T_h = 8.0\%$. The flickering value is 23%. Note that before the polymerization, the flickering is almost independent of the monomer concentration.

The FFS cells are then irradiated by UV to polymerize the monomer. After polymerization, the electro-optical properties of the cell are measured again. The transmittance-voltage curves of the cells are shown in Fig. 3(a). When the monomer concentration is increased from 0 to 3%, the driving voltage (for the maximum transmittance) increases from 7 V to 11 V and the maximum transmittance decreases slightly because of the formed polymer which tends to keep the LC in voltage-off state. The increase of the driving voltage is modest. The square wave voltage with the frequency of 5 Hz and the amplitude for 20% of the maximum transmittance is applied to the cells to study their flickering. The results are shown in Fig. 3(b). The flickering is significantly reduced by the polymer network. When the monomer concentration is increased from 0 to 3%, the flickering value under 5 Hz decreases from 23% to 5%.
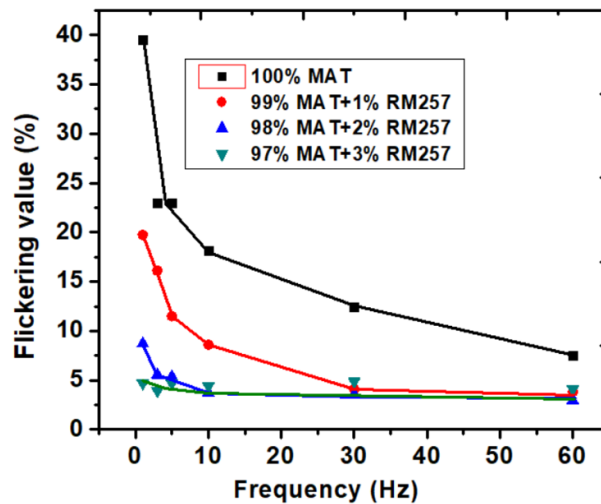

Fig. 4. Flickering value of the cells after polymerization as a function of the frequency of the applied voltage. The lines are guide to the eye.

We also study the flickering of the cells after polymerization under voltages with various frequencies. The results are shown in Fig. 4. For the cell without polymer, when the frequency is decreased from 60 Hz to 1 Hz, the flickering value is increased from 10% to 40%. The flickering under all the frequencies is decreased for the cells with polymer networks. For the cell with 3% monomer, when the frequency is decreased from 60 Hz to 1 Hz, the flickering value remains at 3% down to the frequency of 10 Hz, and then slightly increases to 5% at 1 Hz. The reduction of the flickering is remarkable. When the flickering value is 3%, the absolute transmittance is only changed by 0.2%, which is not observable for human eye.

Image flickering also depends on the switching time of the display. If the viscosity coefficient of the LC is large, the switching time is long and the flickering is small. In order to
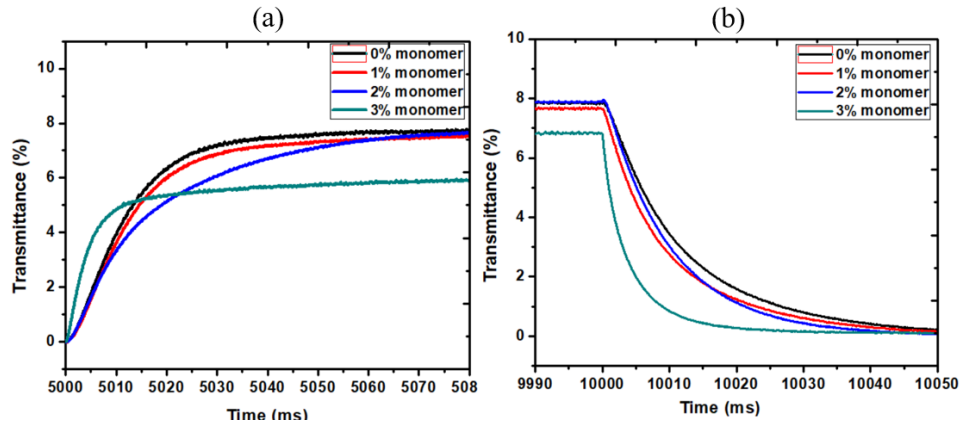

Fig. 5. Transmittance vs. time curves of the polymer stabilized FFS displays (after polymerization). The percentages shown are the monomer concentrations. (a) Turn-on curve, (b) Turn-off curve.

Table 1. Turn-on and turn-off times of the polymer stabilized FFS displays

Monomer concentration	0%	1%	2%	3%
Applied voltage (V)	2.6	2.6	3.6	4.7
Turn-on time (ms)	22	24	39	13
Turn-off time (ms)	28	25	22	11

see whether the switching time plays a role in the reduction of the flickering in the polymer stabilized displays, we measure their switching time. The transmittance-time curves of the polymer stabilized displays are shown in Fig. 5. The turn-on and turn-off times of the displays (after polymerization) are listed in Table 1. In the measurement of the response times, the applied voltage is the voltage which produces 20% of the maximum transmittance. The applied voltages for the cells with different monomer concentrations are also listed in Table 1. For the cells with 1% and 2% monomer, the turn-off time decreases slightly. For the cell with 3% monomer, the turn-off time decreases more. The decrease of the turn-off time would increase the flickering value. Our experimental result shows the flickering decreases monotonically with the monomer concentration. This result rules out the possibility that the flickering is reduced by the switching time. The behavior of the turn-on time is abnormal: it increases first and then decreases with the monomer concentration. The turn-on time depends on both the polymer network and the applied voltage. On one hand when the monomer concentration is increased, the aligning effect of the formed polymer network becomes stronger, which tends to keep the LC in the dark (voltage-off) state, and thus increases the turn-on time. On the other hand when the applied voltage is increased, the turn-on time decreases. In the measurement, the applied voltage is different for cells with different monomer concentrations. The state of the LC is different when different voltages and

monomer concentrations are used. It is difficult to quantitatively describe the relation between the monomer concentration and the response times.

We also study the aligning effect of the polymer stabilized FFS cells under a polarizing optical microscope. The microphotographs of the cell with 2% monomer are shown in Fig. 6. The texture of the cell at 0 V is shown in Fig. 6(a), where the polarizer is parallel to the alignment layer rubbing direction. It is uniformly dark and no light leakage, indicating the LC is uniformly aligned along the rubbing direction and the polymer network does not cause any misalignment. When the cell is rotated 45°, the texture is shown in Fig. 6(b). It is still uniform except becomes bright. When 3.6 V is applied, the texture is shown in Fig. 6(c), where the polarizer is parallel to the alignment layer rubbing direction. The periodical brightness variation is caused by the interdigitated electrodes. Furthermore, there are some non-uniformities which is produced by the polymer network whose location is random.
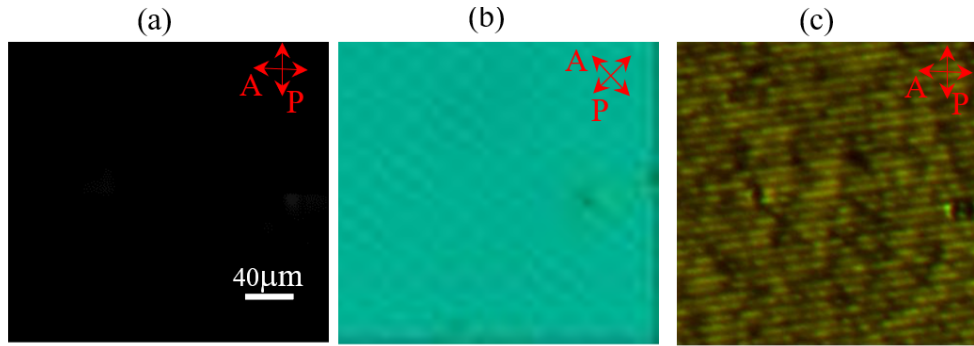

Fig. 6. Microphotographs of the polymer stabilized FFS cells with 2% monomer. (a) at 0 V and polarizer parallel to rubbing direction. (b) at 0 V and polarizer parallel making 45° to rubbing direction. (c) at 3.6 V and polarizer parallel to rubbing direction.

3. Simulation and results

In order to understand the mechanism of how the flickering is reduced by the polymer stabilization, we carry out a simulation study of the polymer stabilized FFS display. The LC configuration is determined by the following factors. The first factor is the dielectric interaction between the LC and the externally applied electric field $\vec{E}$. Its contribution to the free energy of the system is given by

$$f_{\text{dielectric}} = -\frac{1}{2}\varepsilon_o\Delta\varepsilon(\vec{E}\cdot\vec{n})^2, \tag{2}$$

where $\Delta\varepsilon$ and $\vec{n}$ are the dielectric anisotropy and director of the LC, respectively. This interaction is not sensitive to the polarity of the electric field. The applied electric field tends to align the LC parallel or antiparallel to it.

The electric field produced by the interdigitated electrodes in the FFS cell is not uniform. Furthermore the direction of the LC director on the surfaces of the cell is anchored by the alignment layers. The resulted LC director configuration is not uniform, but varies in space. The deformation of the LC director costs energy, which is the second factor affecting the LC configuration. The contribution to the free energy of the system is given by

$$f_{\text{elastic}} = \frac{1}{2}K_{11}(\nabla\cdot\vec{n})^2 + \frac{1}{2}K_{22}(\vec{n}\cdot\nabla\cdot\vec{n})^2 + \frac{1}{2}K_{33}(\vec{n}\times\nabla\times\vec{n})^2, \tag{3}$$

This factor is against the reorientation induced by the electric field.

Because of the LC director deformation, the permanent dipoles of the LC molecules may point in a certain direction, which results in a net electric polarization and is known as the

flexoelectric effect. The electric polarization will interact with the externally applied electric field and its contribution to the free energy is given by [3,24]

$$f_{\text{flexo}} = -[e_s(\vec{n}\nabla \cdot \vec{n}) + e_b(\vec{n}\times\nabla\times\vec{n})]\cdot\vec{E}, \tag{4}$$

where e_s and e_b are the splay and bend flexoelectric coefficients, respectively, of the LC. This flexoelectric interaction is the third factor that affects the LC configuration. This interaction is sensitive to the polarity of the applied electric field. When voltages with the same amplitude but different polarities are applied to the electrodes, their effects on orientation of the LC are different and produce the flickering.

The last factor is the interaction between the LC and the polymer network dispersed in the LC. The polymer network is formed in the voltage-off state where the LC is uniformly aligned parallel to the easy direction of the alignment layer. The polymer network tends to maintain the LC in the voltage-off state. When the LC reorients under the influence of the externally applied electric field, the interaction energy between the LC and the polymer network increases and thus is against the reorientation. We can use an effective aligning field $\vec{E}_p$ to represent the aligning effect of the polymer network on the LC and the interaction energy is given by [38]

$$f_{\text{polymer}} = -\frac{1}{2}\varepsilon_0\Delta\varepsilon(\vec{E}_p \cdot \vec{n})^2, \tag{5}$$

Note that in the calculation of $\vec{E}_p$, the dielectric anisotropy $\Delta\varepsilon$ is included in such a way that the interaction energy f_{polymer} is independent of $\Delta\varepsilon$. The free energy density of the system is given by

$$f = f_{\text{dielectric}} + f_{\text{elastic}} + f_{\text{flexo}} + f_{\text{polymer}}, \tag{6}$$

The LC director configuration is calculated by minimizing the total free energy of the system. In the simulation the following physical parameters are used: the elastic constants are $K_{11} = 11.8\,pN$, $K_{22} = 6.1\,pN$ and $K_{33} = 12.4\,pN$; the dielectric anisotropy is $\Delta\varepsilon = 5.5$; the cell thickness is 4.5 μm; electrode width is 3 μm; the gap between electrode is 5 μm; and the rotational viscosity coefficient is 71mPa·s. The effective aligning field $\vec{E}_p$ of the polymer network, depending on the polymer concentration and morphology, is given by [38]

$$E_P = (\pi c K / 2\varepsilon_o\Delta\varepsilon)^{1/2} / R, \tag{7}$$

where R is the radius of the fibril of the polymer network, c is the concentration of the polymer network and K is the average elastic constant. For example, when $R = 0.2\,\mu m$, $K = 10^{-11}\,N$ and $c = 1\%$, then $E_P \approx 0.2\,\text{V}/\mu\text{m}$. The flexoelectric coefficients are unknown and are treated as fitting parameters in our simulation. The best fit is obtained with $e_s = 6\,pC/m$ and $e_b = 9\,pC/m$ [39].
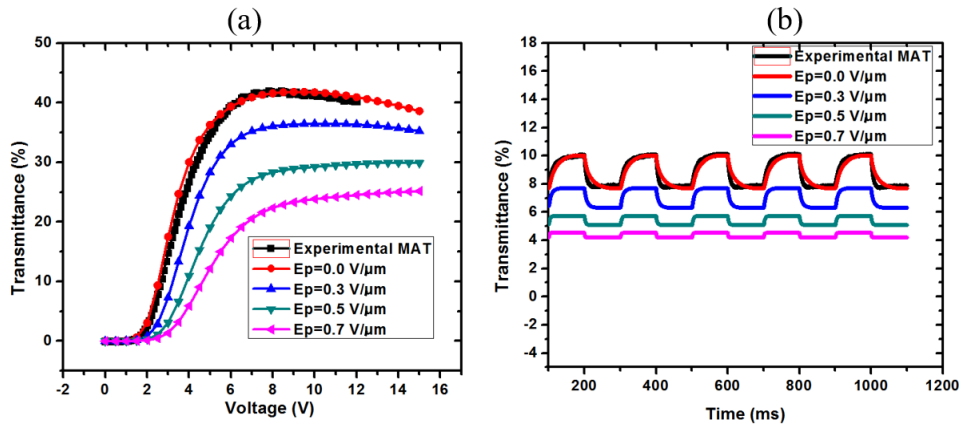
Fig. 7. Simulated electro-optical properties if the FFS displays under various polymer aligning fields. (a) Transmittance-voltage curves, (b) Transmittance-time

We use computer simulation to study the effect of the polymer network aligning field on the electro-optical properties of the polymer stabilized FFS display. We use lab-developed simulation software coded in Matlab. The simulation region (8×5 μm^2) is divided into a mess consisting of 32×25 lattice sites. Relaxation method is used, where the sum of the elastic, dielectric and flexoelectric torques is balanced by the rotational viscosity torque. Figure 7(a) shows the simulated transmittance-voltage curves. As the polymer aligning field is increased, the maximum transmittance decreases slightly and the driving voltage increases slightly, agreeing with the experimental results. Figure 7(b) shows the simulated transmittance-time curves under 5 Hz square wave voltage. The amplitude of the voltage wave is the corresponding voltage for 20% of the maximum transmittance of the display. When the polymer aligning field is increased, the maximum transmittance decreases and the voltage to obtain 20% of the maximum transmittance increases. The flickering decreases with the polymer aligning field. When the aligning field is $E_P = 0.0$ V / μm, the flickering value is 23%. When the aligning field is $E_P = 0.7$ V / μm, the flickering value decreases to 7%.

The molecular structure of the monomer is similar to that of the LC molecule. It is unlikely that the monomer with such low concentrations significantly changes the flexoelectric coefficients. We speculate that the polymer network reduces the LC director deformation in the voltage-on state, because the polymer network favors the voltage-off state where there is no deformation of the LC director. In order to confirm our speculation, we calculate the LC director deformations in the polymer stabilized FFS display under various polymer network aligning fields. The coordinate has its z axis perpendicular to the cell substrate and the x axis perpendicular to the stripe electrode as shown in Fig. 1. When a voltage is applied to the interdigitated electrodes, the generated electric field is on the xz plane. The LC is rotated by the electric field through the dielectric interaction. Because of the non-uniform electric field (whose strength and direction vary in space) and the anchoring effect of the alignment layers on the cell surface, the LC director is not uniform but deformed in space. The deformation of the LC director produces an electric polarization which interacts with the applied electric field and causes the flickering. The flickering caused by the flexoelectric effect only depends on the following deformation parameters:
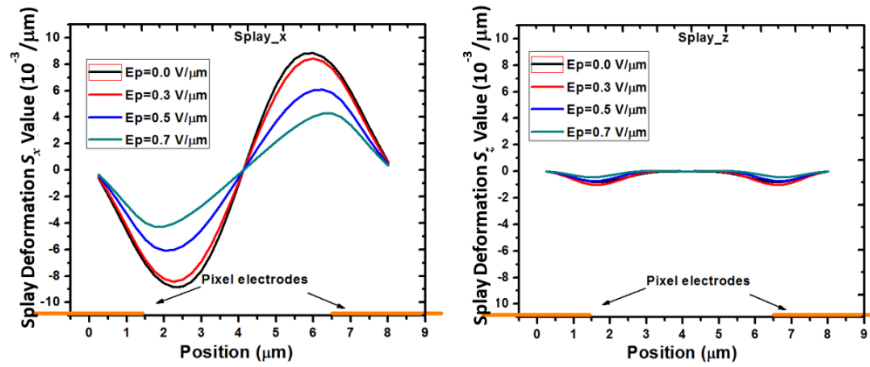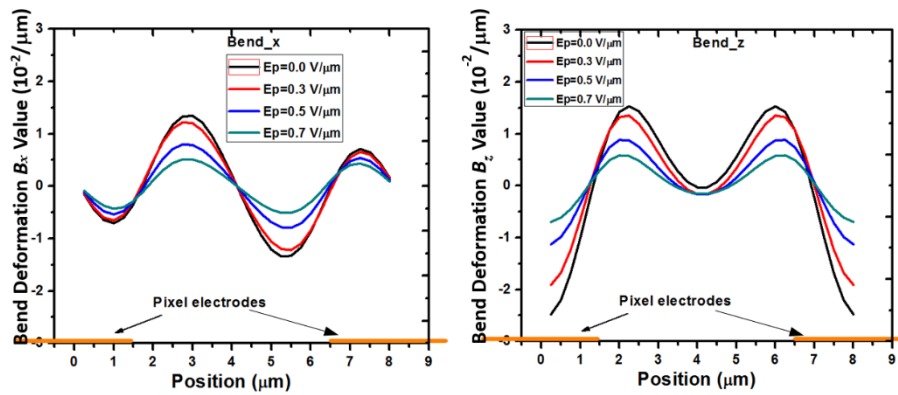
Fig. 8. Simulated splay deformation parameters

Fig. 9. Simulated bend deformation parameters

$$S_x = [\vec{n}(\nabla \cdot \vec{n})]_x = (\frac{\partial n_x}{\partial x} + \frac{\partial n_y}{\partial y} + \frac{\partial n_z}{\partial z})n_x \qquad (8)$$

$$S_z = [\vec{n}(\nabla \cdot \vec{n})]_z = (\frac{\partial n_x}{\partial x} + \frac{\partial n_y}{\partial y} + \frac{\partial n_z}{\partial z})n_z \qquad (9)$$

$$B_x = (\vec{n} \times \nabla \times \vec{n})_x = -n_x \frac{\partial n_x}{\partial x} - n_y \frac{\partial n_x}{\partial y} - n_z \frac{\partial n_x}{\partial z} \qquad (10)$$

$$B_z = (\vec{n} \times \nabla \times \vec{n})_z = -n_x \frac{\partial n_z}{\partial x} - n_y \frac{\partial n_z}{\partial y} - n_z \frac{\partial n_z}{\partial z} \qquad (11)$$

The results are shown in Fig. 8 and 9, where only the effects of the electric field through the dielectric interaction and the polymer network are considered. Note that different scales are used for the vertical axis in Fig. 8 and 9. The bend deformation is much larger than the splay deformation [39]. The voltage used is the value corresponding to 20% of the maximum transmittance. As the polymer aligning field is increased from $0.0V / \mu m$, the deformation parameters, except S_z, decrease monotonically. S_z increases first and then decreases, which is due to the increase of the applied voltage required to obtain the 20% of the maximum transmittance. This result confirms our speculation that the polymer network suppresses the LC director deformation, and thus reduces the flickering.

4. Discussion and conclusion

We experimentally demonstrated that the image flickering in FFS display can be significantly reduced by polymer stabilization. When 3% polymer is added to the LC host, the flickering value under 5 Hz reduced from 23% to 5%. With this polymer concentration, the driving voltage is still below 11 V, which is compatible with TFT technology. Furthermore the turn-off time is reduced by a factor of 3. An ideal display should be able to show both fast video rate images and static images. Fast response time is necessary for the display to show fast video rate image under high driving frequencies, and low flickering value is required for the display to show static images under low driving frequencies.

One important issue with polymer stabilized LC displays is light scattering. If the refractive indices of the polymer network are not matched to those of the LC, the phase separated polymer network may cause light scattering. In the dark state, the scattering depolarizes the linearly polarized incident light and causes light leakage, and thus decreases the contrast ratio of the display. In our experiment, the mesogenic monomer and LC are carefully chosen and the polymerization condition is optimized to minimize the light scattering [37]. We use the monomer RM257 with which high contrast ratio is achieved, as shown in Fig. 3(a). In the selection of monomer, another important property should be considered is its solubility in LC host, which may affect the electro-optical property of the polymer stabilized LC display. If the monomer is in nematic phase at room temperature, its solubility in the nematic host would be better. Furthermore the size of the formed polymer network is more uniform and the driving voltage is lower [40].

There are some trade-off to use the polymer stabilization. Usually the driving voltage is increased, which decreases the energy efficiency of the display. The maximum transmittance is decreased slightly, which also decreases the energy efficiency of the display. Further research is needed to minimize these effects.

In production, the polymer stabilization can be done by adding a small amount of mesogenic monomer to the LC host and then irradiating the display panel at room temperature in the absence of applied voltage under UV light [41]. Therefore, this method can be implemented in the current main stream manufacturing.

We also used computer simulation to investigate the mechanism of how the polymer stabilization reduces the image flickering. We found that the spatial variation of the liquid crystal in the voltage-on state is decreased by the dispersed polymer network. Thus the flexoeletric effect, which is responsible for the flickering, is significantly suppressed.

References

1. J.-H. Lee, D. N. Liu, and S.-T. Wu, *Introduction to flat panel displays* (John Wiley & Sons, Ltd, 2008).
2. E. Lueder, *Liquid Crystal Displays* (John Wiley & Sons, Ltd, 2010).
3. D.-K. Yang and S.-T. Wu, *Fundamentals of Liquid Crystal Devices,* 2νδ εδ. (John Wiley & Sons, Ltd, 2014).
4. M. Schadt and W. Helfrich, "Voltage-dependent optical activity of a twisted nematic liquid crystal," Appl. Phys. Lett. **18**(4), 127–128 (1971).
5. R. A. Soref, "Field effects in nematic liquid crystals obtained with interdigital electrodes," J. Appl. Phys. **45**(12), 5466–5468 (1974).
6. M. F. Schiekel and K. Fahrenschon, "Deformation of nematic liquid crystals with vertical orientation in electrical fields," Appl. Phys. Lett. **19**(10), 391–393 (1971).
7. A. Takeda, S. Kataoka, T. Sasaki, H. Chida, H. Tsuda, K. Ohmuro, Y. Koike, T. Sasabayashi, and K. Okamoto, *Super‐High Image Quality Multi‐Domain Vertical Alignment LCD by New Rubbing‐Less Technology*, SID Symp. Dig. Tech. Pap. **29**, 1077 (1998).
8. R. A. Soref, "Field effects in nematic liquid crystals obtained with interdigital electrodes," J. Appl. Phys. **45**(12), 5466–5468 (1974).
9. M. Oh-e and K. Kondo, "Electro-optical characteristics and switching behavior of the in-plane switching mode," Appl. Phys. Lett. **67**(26), 3895–3897 (1995).
10. M. Oh-e and K. Kondo, "Response mechanism of nematic liquid crystals using the in-plane switching mode," Appl. Phys. Lett. **69**(5), 623–625 (1996).
11. M. Ohta, M. Oh-e, and K. Kondo, "Development of super-TFT-LCDs with in-plane switching display mode," Proc of Asia Display **95**, 707–710 (1995).

12. S. H. Lee, S. L. Lee, and H. Y. Kim, "Electro-optic characteristics and switching principle of a nematic liquid crystal cell controlled by fringe-field switching," Appl. Phys. Lett. **73**(20), 2881–2883 (1998).
13. Y. M. Jeon, I. S. Song, S. H. Lee, H. Y. Kim, S. Y. Kim, and Y. J. Lim, "P-165: Optimized electrode design to improve transmittance in the fringe-field switching (FFS) liquid crystal cell," SID Symp. Dig. Tech. Pap. **36**(1), 328–331 (2005).
14. H. S. Choi, J. H. Kim, H. G. Ham, Y. J. Lim, J. M. Lee, H. S. Jin, R. Manda, M. S. Kim, D.-K. Yang, and S. H. Lee, "P-131: Studies on flickering in low frequency driven fringe-field switching (FFS) liquid crystal display," SID Symp. Dig. Tech. Pap. **47**(1), 1610–1613 (2016).
15. C.-S. Lee, H.-S. Choi, H.-G. Ham, H.-S. Yoo, M. Kim, Y.-J. Lim, T.-H. Kim, P. J. Bos, D.-K. Yang, and S.-H. Lee, "P-149: Maximization of transmittance and minimization of image-flickering due to flexoelectric effect in low-frequency driving fringe-field switching (FFS) mode using LCs with negative dielectric anisotropy," SID Symp. Dig. Tech. Pap. **48**(1), 1841–1844 (2017).
16. H. Chen, F. Peng, M. Hu, and S.-T. Wu, "Flexoelectric effect and human eye perception on the image flickering of a liquid crystal display," Liq. Cryst. **42**(12), 1730–1737 (2015).
17. H. Chen, F. Peng, M. Hu, and S. T. Wu, "23-1: Distinguished student paper: Flexoelectric effect on image elickering of fringe field switching LCDs," SID Symp. Dig. Tech. Pap. **47**(1), 274–277 (2016).
18. H. Lee, H. Kim, J. Kim, and J.-H. Lee, "Dependence of image flickering of negative dielectric anisotropy liquid crystal on the flexoelectric coefficient ratio and the interdigitated electrode structure," J. Phys. D Appl. Phys. **49**(7), 075501 (2016).
19. J.-W. Kim, T.-H. Choi, T.-H. Yoon, E.-J. Choi, and J.-H. Lee, "Elimination of image flicker in fringe-field switching liquid crystal display driven with low frequency electric field," Opt. Express **22**(25), 30586–30591 (2014).
20. S.-W. Oh, J.-H. Park, J.-H. Lee, and T.-H. Yoon, "Elimination of image flicker in a fringe-field switching liquid crystal display by applying a bipolar voltage wave," Opt. Express **23**(18), 24013–24018 (2015).
21. S.-W. Oh, J.-H. Park, J.-M. Baek, T.-H. Choi, and T.-H. Yoon, "Effect of electrode spacing on image flicker in fringe-field-switching liquid crystal display," Liq. Cryst. **43**(7), 972–979 (2016).
22. M. Kim, H.-G. Ham, H.-S. Choi, P. J. Bos, D.-K. Yang, J.-H. Lee, and S.-H. Lee, "Flexoelectric in-plane switching (IPS) mode with ultra-high-transmittance, low-voltage, low-frequency, and a flicker-free image," Opt. Express **25**(6), 5962–5971 (2017).
23. M. S. Kim, P. J. Bos, D.-W. Kim, D.-K. Yang, J. H. Lee, and S. H. Lee, "Flexoelectric effect in an in-plane switching (IPS) liquid crystal cell for low-power consumption display devices," Sci. Rep. **6**(1), 35254–35264 (2016).
24. R. B. Meyer, "Piezoelectric effects in liquid crystals," Phys. Rev. Lett. **22**(18), 917 (1969).
25. J. S. Patel and R. B. Meyer, "Flexoelectric electro-optics of a cholesteric liquid crystal," Phys. Rev. Lett. **58**(15), 1538–1540 (1987).
26. F. Castles, S. M. Morris, and H. J. Coles, "Flexoelectro-optic properties of chiral nematic liquid crystals in the uniform standing helix configuration," Phys. Rev. E Stat. Nonlin. Soft Matter Phys. **80**(3), 031709 (2009).
27. L. Komitov, S. T. Lagerwall, B. Stebler, and A. Strigazzi, "Sign reversal of the linear electro-optic effect in the chiral nematic phase," J. Appl. Phys. **76**(6), 3762–3768 (1994).
28. X. Zhou, Y. Jiang, G. Qin, X. Xu, and D.-K. Yang, "Static and dynamic properties of hybridly aligned flexoelectric in-plane-switching liquid-crystal display," Phys. Rev. Appl. **8**(5), 054033 (2017).
29. T. Tsuruma, Y. Goto, A. Higashi, M. Watanabe, H. Yamaguchi, and T. Tomooka, "Novel image sticking model in the fringe field switching mode based on the flexoelectric effect," Proc. Eurodisplay **11**, 13 (2011).
30. I. H. Jeong, I. W. Jang, D. H. Kim, J. S. Han, B. V. Kumar, and S. H. Lee, "Investigation on flexoelectric effect in the fringe field switching mode," SID Symp. Dig. Tech. Pap. **44**, 1368–1371 (2013).
31. D.-J. Lee, G.-Y. Shim, J.-C. Choi, J.-S. Park, J.-H. Lee, J.-H. Baek, H. C. Choi, Y. M. Ha, A. Ranjkesh, and H.-R. Kim, "Transient flickering behavior in fringe-field switching liquid crystal mode analyzed by positional asymmetric flexoelectric dynamics," Opt. Express **23**(26), 34055–34070 (2015).
32. M. S. Kim, P. J. Bos, D.-W. Kim, C.-M. Keum, D.-K. Yang, H. G. Ham, K.-U. Jeong, J. H. Lee, and S. H. Lee, "Field-symmetrization to solve luminance deviation between frames in a low-frequency-driven fringe-field switching liquid crystal cell," Opt. Express **24**(26), 29568–29576 (2016).
33. D. J. Broer, "Liquid crystalline networks formed by photoinitiated chain cross-linking" in Liquid Crystals in Complex Geometries, ed. G.P. Crawford and S. Zumer (Taylor & Francis, 1996).
34. I. Dierking, "Recent developments in polymer stabilised liquid crystals," Polym. Chem. **1**(8), 1153–1159 (2010).
35. D.-K. Yang, "Polymer stabilized liquid crystal displays," in Progress in liquid crystal science and technology, ed. H-S. Kwok, S. Naemura and H. L. Ong, (World Scientific, 2013).
36. R. Q. Ma and D.-K. Yang, "Freedericksz transition in polymer-stabilized nematic liquid crystals," Phys. Rev. E Stat. Phys. Plasmas Fluids Relat. Interdiscip. Topics **61**(2), 1567–1573 (2000).
37. X.-C. Zhou, G.-K. Qin, Y.-M. Dong, and D.-K. Yang, "Fast switching and high-contrast polymer-stabilized IPS liquid crystal display," J. Soc. Inf. Disp. **23**(7), 333–338 (2015).
38. D.-K. Yang, Y. Cui, H. Nemati, X.-C. Zhou, and A. Moheghi, "Modeling aligning effect of polymer network in polymer stabilized nematic liquid crystals," J. Appl. Phys. **114**(24), 243515 (2013).
39. Y. Jiang, X. Zhou, G. Qin, X. Xu, S.-H. Lee, and D.-K. Yang, "81-3: Effects of flexoelectricity and ion on the flicker of fringe field switching liquid crystal display," SID Symp. Dig. Tech. Pap. **49**(1), 1095–1098 (2018).

40. L. De Sio, P. F. Lloyd, N. V. Tabiryan, and T. J. Bunning, "Hidden gratings in holographic liquid crystal polymer-dispersed liquid crystal films," Appl. Mater. Interfaces **10**, 13107–13112 (2018).
41. C.-H. Pai, T.-Y. Cho, S.-C. Tsai, C.-Y. Chiu, T.-S. Chen, H.-C. Lin, J.-J. Su, and A. Lien, "Fast-response study of polymer-stabilized VA-LCD," J. of SID **18**, 960–967 (2012).